THE JOURNAL OF BIOLOGICAL CHEMISTRY Vol. 280, No. 7, Issue of February 18, pp. 5892–5901, 2005
Printed in U.S.A.

Curcumin Inhibits Formation of Amyloid β Oligomers and Fibrils, Binds Plaques, and Reduces Amyloid *in Vivo**

Received for publication, April 28, 2004, and in revised form, December 6, 2004
Published, JBC Papers in Press, December 7, 2004, DOI 10.1074/jbc.M404751200

Fusheng Yang‡§, Giselle P. Lim‡§, Aynun N. Begum‡§, Oliver J. Ubeda‡§, Mychica R. Simmons‡§, Surendra S. Ambegaokar‡§, Pingping Chen‡§, Rakez Kayed¶, Charles G. Glabe¶, Salley A. Frautschy‡§‖, and Gregory M. Cole‡§‖**

From the ‡Department of Medicine, UCLA, Los Angeles, California 90095, the §Greater Los Angeles Veterans Affairs Healthcare System, Geriatric Research Education and Clinical Center, Sepulveda, California 91343, the ‖Department of Neurology, UCLA, Los Angeles, California 90095, and the ¶Department of Molecular Biology and Biochemistry, University of California, Irvine, California 92697-3900

Alzheimer's disease (AD) involves amyloid β (Aβ) accumulation, oxidative damage, and inflammation, and risk is reduced with increased antioxidant and anti-inflammatory consumption. The phenolic yellow curry pigment curcumin has potent anti-inflammatory and antioxidant activities and can suppress oxidative damage, inflammation, cognitive deficits, and amyloid accumulation. Since the molecular structure of curcumin suggested potential Aβ binding, we investigated whether its efficacy in AD models could be explained by effects on Aβ aggregation. Under aggregating conditions *in vitro*, curcumin inhibited aggregation (IC_{50} = 0.8 μM) as well as disaggregated fibrillar Aβ40 (IC_{50} = 1 μM), indicating favorable stoichiometry for inhibition. Curcumin was a better Aβ40 aggregation inhibitor than ibuprofen and naproxen, and prevented Aβ42 oligomer formation and toxicity between 0.1 and 1.0 μM. Under EM, curcumin decreased dose dependently Aβ fibril formation beginning with 0.125 μM. The effects of curcumin did not depend on Aβ sequence but on fibril-related conformation. AD and Tg2576 mice brain sections incubated with curcumin revealed preferential labeling of amyloid plaques. *In vivo* studies showed that curcumin injected peripherally into aged Tg mice crossed the blood-brain barrier and bound plaques. When fed to aged Tg2576 mice with advanced amyloid accumulation, curcumin labeled plaques and reduced amyloid levels and plaque burden. Hence, curcumin directly binds small β-amyloid species to block aggregation and fibril formation *in vitro* and *in vivo*. These data suggest that low dose curcumin effectively disaggregates Aβ as well as prevents fibril and oligomer formation, supporting the rationale for curcumin use in clinical trials preventing or treating AD.

The 4-kDa (40–42-amino acid) amyloid-β peptide (Aβ)[1] is derived from the amyloid precursor protein (APP) through sequential proteolysis by the aspartyl protease β-secretase and presenilin-dependent γ- secretase cleavage (1). Mutations at the cleavage sites in APP or in presenilin that increase production or aggregation of Aβ provide a compelling argument for a central role for Aβ aggregation in the pathogenesis of Alzheimer's disease (AD). The progressive accumulation of Aβ aggregates is widely believed to be fundamental to the initial development of neurodegenerative pathology and to trigger a cascade of events such as neurotoxicity, oxidative damage, and inflammation that contribute to the progression of AD (2–5). Therefore, many therapeutic efforts are targeted at reducing Aβ production, including inhibiting secretase, increasing Aβ clearance with amyloid vaccines, or blocking Aβ aggregation (with antibodies, peptides, or small organic molecules that selectively bind and inhibit Aβ aggregate and fibril formation).

Aβ fibrillization involves formation of dimers and small oligomers followed by growth into protofibrils and fibrils via a complex multistep-nucleated polymerization. Polymerizing Aβ fibrils and intermediates can be stained by amyloidophilic dyes such as Congo Red (CR) (6). Congo Red can inhibit the toxic and inflammatory activity of polymerizing Aβ (7, 8) and prevent the natural oligomer formation found at low Aβ concentrations (9). However, CR is toxic and negatively charged and therefore poorly brain-penetrant (10).

Curcumin (diferulomethane) is a low molecular weight molecule with potent antioxidant and anti-inflammatory activities that has a favorable toxicity profile and is under development as a potential cancer chemotherapeutic agent (11). Our previous results demonstrated that chronic dietary curcumin lowered Aβ deposition in 16-month-old APPsw transgenic mice (Tg2576) (12). However, it remains unresolved whether curcumin was reducing plaques in *vivo* in part by effects on aggregation. As shown in Fig. 1, curcumin has a structure similar to Congo Red but with the charge replaced by polar groups like the brain-permeable compound chrysamine G (10, 13). It is also similar to RS-0406, a novel compound selected from a screen of 113,000 compounds as a potent inhibitor of Aβ oligomer formation (14). We hypothesized that, like these polar Aβ binding compounds, curcumin might be able to cross the blood-brain barrier and bind to amyloid and related aggregates. Therefore, in these studies, we used an *in vitro* model of Aβ fibrillization

* This work was supported by the Siegel Life Foundation (to S. A. F. and G. M. C.), National Institute of Neurological Disorders and Stroke Grant NS43946 (to G. M. C.), a Veterans Affairs Merit award (to G. M. C.), the Alzheimer Association (to G. M. C.), and UCLA Alzheimer's Disease Research Center Grant P50 AG 16570 (to G. M. C. and S. A. F.). The costs of publication of this article were defrayed in part by the payment of page charges. This article must therefore be hereby marked "*advertisement*" in accordance with 18 U.S.C. Section 1734 solely to indicate this fact.

** To whom correspondence should be addressed: Greater Los Angeles VA Healthcare System GRECC11E, UCLA Depts. of Medicine and Neurology (SFVP), 16111 Plummer St., Sepulveda, CA 91343. Tel.: 818-891-7711 (ext. 9949); Fax: 818-895-5835; E-mail: gmcole@ucla.edu.

[1] The abbreviations used are: Aβ, amyloid β; APP, amyloid precursor protein; AD, Alzheimer's disease; CR, Congo Red; dH_2O, distilled H_2O; BSA, bovine serum albumin; PBS, phosphate-buffered saline; ELISA, enzyme-linked immunosorbent assay; Tricine, *N*-[2-hydroxy-1,1-bis(hydroxymethyl)ethyl]glycine; ANOVA, analysis of variance; EM, electron microscopy; LDH, lactate dehydrogenase; NSAID, nonsteroidal anti-inflammatory drug; HFIP, hexafluoroisopropanol.

to show that curcumin can bind amyloid to inhibit Aβ aggregation as well as fibril and oligomer formation with dosing at achievable levels. We also demonstrate that curcumin can label plaques *in vitro* and *in vivo*, block toxicity of oligomers *in vitro*, and significantly reduce amyloid levels in aged Tg2576 mice (22 months old) fed a curcumin diet beginning at 17 months after established amyloid deposition.

EXPERIMENTAL PROCEDURES

Materials

Aβ40 and Aβ42 peptides were purchased from the laboratory of Dr. Charles Glabe (University of California, Irvine, CA) and American Peptide (Sunnyvale, CA). Aβ fragment peptides 1–13, 1–28, 25–35, 34–40, and 37–42 were purchased from Bio-Synthesis (Lewisville, TX), and Aβ 12–28 was purchased from American Peptide Company. Aβ 8–17, 14–24, 17–24, and 17–28 were purchased from Quality Control Biochemicals (Hopkinton, MA). Curcumin, naproxen, and ibuprofen were purchased from Cayman Chemicals (Ann Arbor, MI). Stocks of curcumin, naproxen, and ibuprofen (5 mM) were dissolved in 100% ethanol and stored at −80 °C. A 5 mM stock of Congo Red was prepared in dH_2O immediately before use. The 6E10 antibody (Aβ 1–17) was purchased from Signet Labs, and the A11 antibody was generously provided by C. Glabe (University of California, Irvine). All other reagents were from Sigma.

Curcumin Staining of Human AD and Tg2576 Mouse Brain Sections (in Vitro)

Just before use, curcumin was diluted from 2.5 mM to 50 nM in 0.1 M TBS (pH 7.4) containing 3% BSA with 0.5% Tween 20. Thioflavin S (1%) was freshly prepared in dH_2O, stirred for 0.5 h, and filtered. Human AD hippocampus was fixed in buffered formalin and snap-frozen. Tg2576 mice (22 months old) were perfused with Hepes buffer and protease inhibitors (15), and brains were removed, fixed in buffered formalin, and snap-frozen. Both brains were cryosectioned at 12 μm and stored at −70 °C. Sections were warmed to room temperature for 10 min and dipped in 75% ethanol, treated with 0.3% Triton X-100 and 0.1 M TBS (pH 7.4) containing 3% BSA with 0.5% Tween 20 for 10 min each. Different concentrations of curcumin were applied to sections for 1 h at 37 °C in a humidified chamber. Sections were washed in TBS three times, rinsed once in dH_2O, and coverslipped with fluorescent mounting medium. Adjacent sections were stained with 1% thioflavin S for 10 min at room temperature and dipped for 1 min in 75% ethanol, 95% ethanol, 100% ethanol, 95% ethanol, and 75% ethanol before rinsing in dH_2O. All sections were examined and photographed with a fluorescence microscope using fluorescein isothiocyanate optics.

In Vivo Curcumin Treatments and Labeling in Tg2576 Mice

Groups of APPsw Tg2576 transgenic mice raised on Purina 5015 breeder chow were placed on 500 ppm curcumin (Sabinsa, Piscataway, NJ) or control safflower oil-based test diets (TD#02347 and TD#02346, respectively; Harlan Teklad) and aged until 22 months. A curcumin stock solution was diluted 1:100 into sterile PBS. Three 22-month-old Tg2576 mice (50 g body weight) were anesthetized with 25 mg/ml nembutal (intraperitoneally). One mouse on the chronic 500 ppm curcumin diet was injected with 200 μl of curcumin/PBS into the right carotid artery over a 5-min period. Because blood volume for a 50-g mouse was estimated to be about 4 ml (80 ml/kg × 0.05 kg), we expected blood levels of curcumin to reach ~2 μM. The other two mice were injected with PBS only as a control, and one of these mice had also received the 500-ppm curcumin diet. After 1 h, the mice were perfused as described previously (15). Brains were removed and snap-frozen in 2-methylbutane chilled by liquid nitrogen. Freshly cut cryosections (12 μm) were air-dried for 10 min in the dark and coverslipped with VECTASHIELD mounting medium for fluorescence protection (Vector Laboratories, Burlingame, CA). Sections were examined and photographed with a Nikon Microphot-Fx fluorescence microscope using a fluorescein isothiocyanate filter set.

Measurement of in Vivo Amyloid Levels

Image Analysis of Plaque Pathology—Plaque burden was assessed using a characterized polyclonal antibody against Aβ 1–13 (DAE) (15). Coronal sections were made through anterior (bregma; −1.00 to −1.46 mm), middle (bregma; −1.58 to −2.30 mm), and posterior hippocampus (bregma; −2.46 to −3.16 mm) of control (n = 6) and curcumin-treated mice (n = 8). Immunolabeling was examined in various cortical and hippocampal areas of animals, and image analysis was performed as described previously (12, 15).

Amyloid Extracts and Assays—Amyloid levels were evaluated in the cortex of control (n = 6) and curcumin-fed (n = 4) Tg2576 mice. Samples were processed in TBS and lysis buffer (detergent) as described previously (16). Detergent-insoluble pellets from cortex were sonicated in 8 volumes of 5 M guanidine, 50 mM Tris-HCl and solubilized by agitation at room temperature for 3–4 h. Guanidine-soluble extracts were diluted 1:10,000 with TBS containing 5% BSA and 1× protease inhibitor mixture (Calbiochem) and assayed for total Aβ by ELISA as described previously (17).

Disaggregation and Inhibition of Aβ Aggregation with Curcumin

Inhibition of Aggregation—Aβ40 was dissolved at 1 mg/ml in dH2O, and curcumin stock was diluted in 0.1 M TBS with 0.02% Tween 20. Aβ40 (100 μg/ml) was mixed a 1:1 volume ratio with curcumin in Eppendorf tubes and incubated for 6 days at 37 °C. Final concentrations of Aβ40 were 50 μg/ml (11.6 μM), and curcumin concentrations were 0, 0.125, 0.25, 0.5, 1, 2, 4, and 8 μM.

Disaggregation of Preformed Fibrils—Aβ40 (100 μg/ml) was incubated for 3 days at 37 °C to generate fibrils. Preformed fibrils were mixed with the same concentrations of curcumin as above for an additional 3 days at 37 °C.

At the end of both incubations, an aliquot (3 μl) was taken from each tube for electron microscopy (EM) analysis. The remaining Aβ solution was assayed for aggregates using the 6E10/6E10 sandwich ELISA.

6E10/6E10 Aggregation ELISA—To determine the relative amount of aggregated Aβ, the monoclonal antibody 6E10 was used for both detection and capture as described by Howlett *et al.* (17). Briefly, 96-well plates were coated with 3 μg/ml 6E10 in 55 mM sodium bicarbonate buffer (pH 9) at 4 °C overnight before wells were blocked for 2 h at room temperature with TBS-Tween 20 (TBS-T; 0.1 M TBS, pH 7.4, 0.02% Tween 20) with 1% BSA. Samples were transferred to the wells, and plates were placed on an orbital shaker (30 rpm) for 2 h at room temperature. After washing four times with TBS-T, biotinylated 6E10 antibody diluted 1:1200 in TBS-T containing 1% BSA was applied to the plate for 1 h at room temperature with shaking. After washing, alkaline phosphatase streptavidin (Vector Laboratories, Burlingame, CA) diluted at 1:4000 in TBS-T with 1% BSA was applied to the plates, followed by the addition of the fluorescent substrate, Attophos (Promega). Fluorescence was measured using a CytoFluor II fluorescence plate reader (excitation 450 nm and emission 580 nm; Applied Biosystems, Foster City, CA).

Efficacy of Curcumin Compared with Other NSAIDs

Aβ 1–40 was dissolved at 1 mg/ml in dH_2O. A 50 μg/ml solution was made with 0, 0.5, 2, or 8 μM curcumin. Naproxen and ibuprofen were tested at 0, 8, 16, and 32 μM. Samples were sealed in Eppendorf tubes and incubated for 6 days at 37 °C. Aβ aggregates were assayed with the 6E10/6E10 ELISA as above. Separate drug-only controls were used to assess possible drug fluorescence interference in the assay.

EM Analysis of Fibril Formation

EM was used to observe inhibition of Aβ fibril formation in disaggregation and aggregation inhibition experiments (see Fig. 5). To determine whether filaments had formed, 3 μl of Aβ peptide solution was applied to 150-mesh copper grids coated with Formvar/carbon film (EM Sciences, Fort Washington, PA) for 30 s. Excess solution on the other side of grids was absorbed with filter paper, grids were stained with one drop of 0.5% filtered uranyl acetate for 20 s, and staining solution was absorbed with filter paper again. After air drying for 4 h or overnight, grids were examined with an electron microscope (TECNAI 10/12; Phillips) at 80 kV.

Curcumin Binding Experiments with Aβ Peptides

Aβ40 and Aβ42 were solubilized in HFIP, dried overnight at room temperature and speed-vacuumed for 10 min (18). Aliquots were stored at −80 °C until they were needed, when they were resolubilized in 20 μl of Me_2SO and dissolved in dH_2O (1 mg/ml). Additional samples of Aβ40, Aβ42, and shorter Aβ peptides were dissolved in dH_2O, whereas Aβ 17–24 was dissolved in Me_2SO. Peptides were aggregated in TBS (0.05 M Tris-HCl, pH 7.4, 75 mM NaCl, 0.025% NaN_3) at 500 μg/ml. Two hundred μl of each peptide solution was sealed in Eppendorf tubes and incubated without shaking at 37 °C for 10 days. After 10 days, an aliquot was removed for EM analysis of structure before solutions from each tube were mixed with curcumin at a final concentration of 1 μM. Samples were incubated at 37 °C for 1 h and then spun at 16,000 × g for

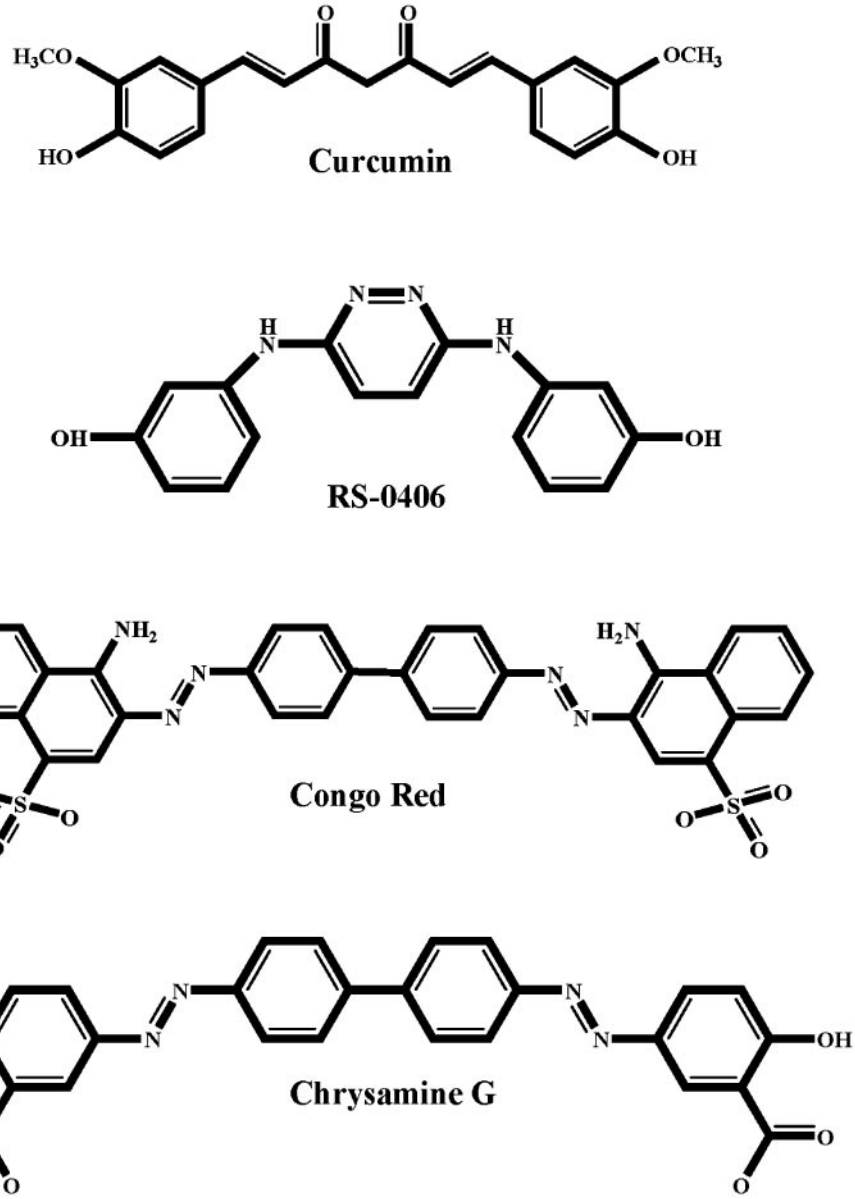

FIG. 1. **Chemical structures of curcumin, RS-0402, Congo Red, and chrysamine G.** Structures (not drawn to scale) have a common theme of two charge or polar groups separated by a hydrophobic bridge.

10 min. To assess curcumin staining of synthetic peptide aggregates, pellets were mixed with 10 μl of dH_2O, smeared to slides, and air-dried for 1 h. Supernatant, spun down after mixing Aβ peptides with 1 μM curcumin, were applied to cryosections of Tg2576 mouse brain (22 months) at 37 °C for 1 h. Slides were coverslipped with anti-quenching mounting medium before examination under a fluorescent microscope (Table I).

Inhibition of Aβ Oligomer Formation

Immunoblot of Curcumin- and Congo Red-treated Aβ42 Oligomers—An aliquot of Aβ42 (0.045 mg) was dissolved in 20 μl of Me_2SO and diluted in Ham's F-12 media without phenol red (BIOSOURCE, Camarillo, CA). Aβ42 (5 μM) was incubated with curcumin (0, 0.25, 1, 4, 16, and 64 μM) or Congo Red (16 and 64 μM) in a 37 °C water bath for 4 h. After the incubation, the samples (72 μl) were spun at 14,000 $\times$ *g* (4 °C for 10 min), and the supernatant (65 μl) was mixed with an equal part of Tricine sample buffer without reducing agents (Bio-Rad). The unaggregated Aβ42 control was not incubated at 37 °C, and after dilution in F-12 medium, it was mixed with sample buffer (no centrifuging) and stored at −20 °C before it was electrophoresed. Samples (30 μl, no boiling) were electrophoresed at 100 V on a 10–20% Tris-Tricine SDS gel, transferred at 100 V for 1 h, and blocked overnight (4 °C) with 10% nonfat milk in PBS plus 0.1% gelatin. The blots were probed with 6E10 (1:2000; 3 h at room temperature), followed by goat anti-mouse horseradish peroxidase (1:10,000; 1 h at room temperature), and developed with ECL.

Dot Blot Assay—Aβ40 oligomer was prepared from HFIP-solubilized Aβ (4 mg/ml, 10–20 min in HFIP at 25 °C). An 80-μl Aβ aliquot was diluted 1:10 with 800 μl of sterile H_2O. The final Aβ concentration was 400 μg/ml or 88 μM. Curcumin was added to Aβ solutions to give final 0, 2, and 16 μM curcumin in 0.01% methanol. After the pH was adjusted (pH 3), the samples were incubated for 2.5 h at 42 °C followed by a 48-h incubation at room temperature with stirring. Samples (500 ng of oligomer) were applied to nitrocellulose membrane in a Bio-Dot apparatus (Bio-Rad). The membrane was blocked with 10% nonfat milk in TBS-T at room temperature for 1 h, washed with TBS-T, and probed with anti-oligomer A11 antibody (19) solution (1:10,000) or 6E10 (1:10,000) in 3% BSA-TBS-T overnight at 4 °C. After washing, it was probed with anti-rabbit horseradish peroxidase- or anti-mouse horseradish peroxidase-conjugated antibody (Pierce) solution (1:12,000) for 1 h at room temperature. The blot was developed with SuperSignal (Pierce) for 2–5 min. Dots were scanned and analyzed with a model GS-700 densitometer using Molecular Analyst software (Bio-Rad).

Toxicity Assays—Confirmation of Aβ oligomer toxicity was performed in human APPSwe neuroblastoma (N2a) cells, which were cultured in 50% Dulbecco's modified Eagle's medium, 50% Opti-MEM (Invitrogen), 5% fetal bovine serum, 200 μg/ml Glutamax. Cells were plated at equal densities (8000 cells/well) with 1.5% bovine calf serum

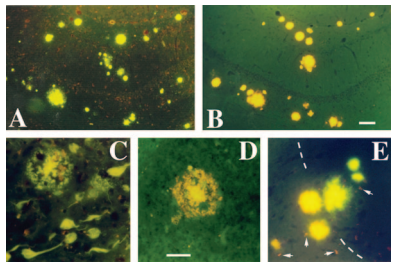

FIG. 2. **Curcumin stains amyloid plaques like thioflavin S in AD and Tg2576 brain sections.** *A* and *B*, adjacent sections from 22-month APPsw Tg2576 brain; *C* and *D*, adjacent sections of AD hippocampus. *E* is from the same section as *B*, but the right half of the field was exposed for 3 min longer than the left half of the field. The *arrows* point to lipofuscin. *A* and *C* are stained with 1% thioflavin S, whereas *B–E* are labeled with curcumin (1 μM). Curcumin fluorochromes produce *orange* to *yellow/green* fluorescent plaques, and thioflavin S results in much better tangle staining. *A* and *B*, *bar*, 80 μm; *C–E*, *bar*, 25 μm.

and maintained at 37 °C in an atmosphere of 5% CO_2. The medium was removed before treatment and replaced with medium containing 70% Dulbecco's modified Eagle's medium, 30% Opti-MEM with 0.1% BSA. An LDH assay was performed on media using the LDH assay toxicity kit (Promega, Madison, WI).

To determine whether curcumin could block this oligomer toxicity, SH-SY5Y human neuroblastoma cells were grown and maintained as described previously (20). Cells were plated at 10,000 cells/well in 96-well plates and were differentiated in low serum Dulbecco's modified Eagle's medium with N_2 supplement and 1×10^{-5} M all-*trans*-retinoic acid for 7 days. The medium was removed and replaced with fresh maintenance medium containing 0.1% BSA. Aβ42 oligomer (100 nM) was added to cells for 48 h at 37 °C with or without 0.1, 1, 2.5, and 5 μM curcumin. After treatment, LDH assay was performed as mentioned above. Cell viability was assayed using the 3-(4,5-dimethylthiazol-2-yl)-2,5-diphenyltetrazolium bromide reduction assay (21), where absorbance was measured at 550 nm. Each data point was determined in triplicate, and the S.D. value did not exceed 5%.

RESULTS

Because curcumin is a fluorochrome, we first compared plaque-associated curcumin fluorescence with that of thioflavin S, using sections from APPsw (Tg2576) mouse brain (Fig. 2, *A*, *B*, and *E*) and AD hippocampus (Fig. 2, *C* and *D*). Like thioflavin S (Fig. 2, *A* and *C*), curcumin brightly labeled amyloid plaques (1 μM; Fig. 2, *B–E*). In AD brain, curcumin labeled plaques with a yellow fluorescence (Fig. 2*D*) similar to thioflavin S in an adjacent section (Fig. 2*C*). Thioflavin S labeled tangles very strongly (Fig. 2*C*), whereas curcumin labeled tangles only weakly or not at all (Fig. 2*D*). Curcumin fluorescence was initially yellow-orange, but with prolonged (>2-min) light exposure, the fluorescence gradually shifted to yellow/green fluorescence. This phenomenon is illustrated in Fig. 2*E*, where the right side of the field was illuminated for 3 min before shifting the field back to make the photoexposure. Color change depended on the intensity of plaque staining and the fluorescent exposure time, and was stable for several weeks at 4 °C. Lipofuscin age pigments in this aged mouse brain (*small arrows*) are orange/red under these thioflavin optics and, unlike curcumin labeling, did not show a fluorescent shift with prolonged illumination. Optimal staining concentrations for curcumin were 0.5–2 μM.

Unlike thioflavin S and Congo Red, curcumin is highly hydrophobic and should readily enter the brain to bind to plaques *in vivo*. In order to evaluate this idea, we injected curcumin (50 μM in 200 μl) or vehicle (PBS) into the carotid artery of aged Tg2576 mice. Mice were sacrificed 1 h later, and unfixed cryosections were immediately prepared from snap-frozen brains. Untreated mice injected with PBS only showed no plaque staining (Fig. 3*A*), but a mouse on a chronic curcumin diet (500 ppm) showed discernable but weak plaque staining when injected

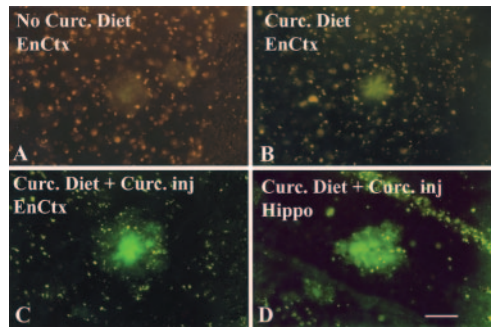

FIG. 3. **Curcumin crosses the blood-brain barrier and binds to plaques *in vivo*.** Tg2576 mice (22 months old) were injected with curcumin or vehicle as described. Mice were perfused 1 h later with protease inhibitor buffer, and brains were removed and snap-frozen. Unfixed cryosections (12 μM) were coverslipped and photographed with fluorescein isothiocyanate filter sets (494 nm/520 nm). *A* is a section from a PBS-injected mouse and shows no plaque staining. *B* is a section from a PBS-injected mouse on chronic curcumin (*Curc*) (500 ppm) for 5 months and shows weaker plaque staining. *C* and *D* are entorhinal cortex (*EnCtx*) and hippocampal (*Hippo*) regions, respectively, from a mouse injected with 50 μM curcumin (200 μl) as described under "Experimental Procedures." Examples of plaque staining are illustrated in these *panels*. *Bar*, 40 μm.

with PBS alone (Fig. 3*B*). Plaques in the curcumin-injected mouse were brightly labeled (Fig. 3, *C* and *D*). These data suggested that curcumin can cross the blood-brain barrier and bind to plaques in transgenic mice after oral feeding or peripheral injection.

Having established that curcumin can stain *in vitro* and *in vivo* amyloid, we sought to test whether it can interfere with Aβ aggregation and its disaggregation. Because curcumin fluoresces over the same wavelengths as thioflavin S, we could not use thioflavin-based assays to quantify amyloid fibrils in curcumin-treated samples, and thioflavin-based assays require high concentrations of Aβ. Therefore, we employed a sandwich ELISA for aggregated Aβ using the same N-terminal Aβ antibody (6E10) for both capture and detection. Aβ40 (final concentration 50 μg/ml) was incubated under fibril-forming conditions with 0–8 μM curcumin. As shown in Fig. 4*A*, Aβ aggregation was significantly inhibited with increasing doses of curcumin, with an approximate IC_{50} of 0.81 μM (*gray circles*; $p < 0.001$). When Aβ was preaggregated for 3 days before incubation with curcumin, increasing doses of curcumin were capable of inducing the disaggregation of preaggregated Aβ40, with an IC_{50} of 1 μM (*filled circles*; $p < 0.005$; Fig. 4*B*). In control experiments, curcumin over this range did not interfere with the Aβ aggregate ELISA and did not interfere with an ELISA with 6E10 as the capture and anti-Aβ 34–40 as the detection (not shown), implying that curcumin did not simply block 6E10 antibody binding.

We also sought to test whether curcumin was better than other NSAIDs at inhibiting Aβ aggregation. Aβ40 (final concentration 50 μg/ml) was incubated with curcumin (0–8 μM), naproxen (0–32 μM), or ibuprofen (0–32 μM) for 6 days at 37 °C. The presence of Aβ aggregates was determined with the 6E10/6E10 ELISA. In this assay, curcumin again showed dose-dependent inhibition of Aβ aggregate formation over the low dose range (Fig. 4*C*), in contrast to naproxen and ibuprofen (Fig. 4, *D* and *E*). These data indicate that although high concentrations of naproxen and ibuprofen can inhibit Aβ aggregation (20), curcumin is a better aggregation inhibitor.

EM Analysis of Inhibition of Fibril Formation—To determine whether curcumin could inhibit the formation of fibrils, EM was used to examine samples of Aβ40 incubated with and without curcumin as described under "Experimental Procedures." Aβ40 (50 μg/ml) incubated for 6 days at 37 °C formed extensive, but less mature fibrils (Fig. 5*A*) than fibrils formed

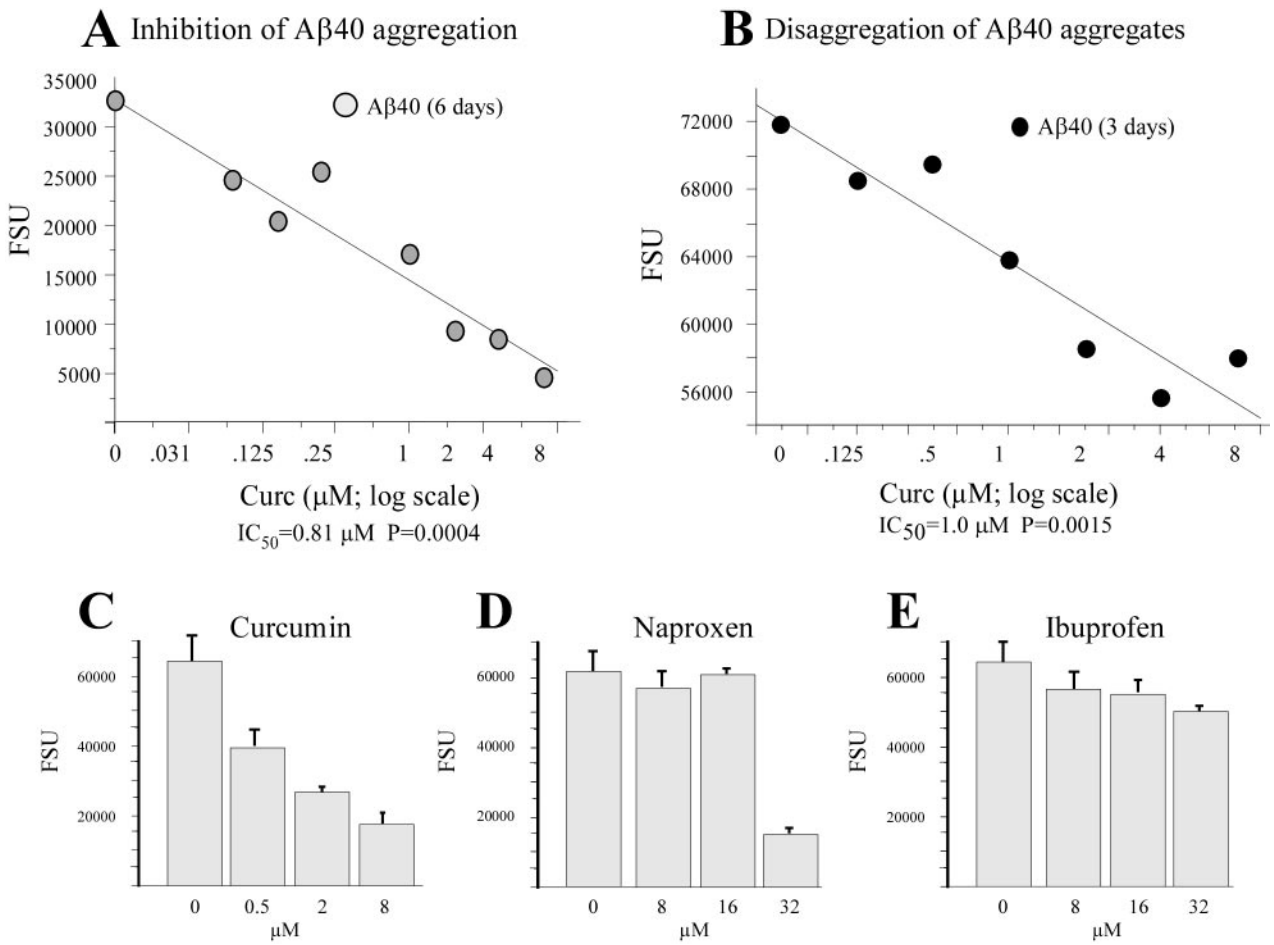

FIG. 4. **Curcumin (*Curc*) inhibits aggregation of Aβ40 and promotes its disaggregation.** The presence of aggregated Aβ was analyzed by ELISA (6E10/6E10), and FSU was plotted against the dose of curcumin (log scale). *A*, inhibition of Aβ40 aggregation. This is a plot of Aβ40 (final concentration 50 μg/ml) incubated with increasing doses of curcumin (0–8 μM) for 6 days at 37 °C. Samples were assayed with 6E10/6E10 sandwich ELISA in triplicate. Curcumin was found to block aggregation of Aβ40, with an IC_{50} of ~0.81 μM (*gray circles*; $p < 0.001$). *B*, induction of disaggregation. The *filled circles* depict a plot of Aβ40 (100 μg/ml) preaggregated for 3 days and then incubated with curcumin (0–8 μM) for 3 days at 37 °C. When Aβ40 was preaggregated, increasing doses of curcumin were able to promote disaggregation of Aβ40, where the IC_{50} was ~1 μM (*closed circles*, $p < 0.005$). *C–E* illustrate that curcumin is a better Aβ aggregation inhibitor than ibuprofen or naproxen. Aβ (50 μg/ml) was incubated with curcumin (0–8 μM) (*C*), naproxen (0–32 μM) (*D*), or ibuprofen (0–32 μM) (*E*). Samples were incubated for 6 days at 37 °C, and the presence of Aβ40 aggregates was determined with 6E10/6E10 ELISA. The *bar graphs* represent the average from three samples, and *error bars* represent S.D.

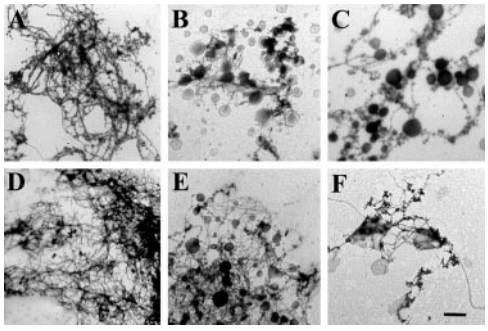

FIG. 5. **EM analysis of curcumin preventing fibril formation and promoting its disaggregation.** A small aliquot (3 μl) was applied to grids for EM analysis. *A–C*, curcumin inhibited Aβ40 aggregation. Aβ40 (50 μg/ml) was allowed to aggregate for 6 days at 37 °C with vehicle alone (*A*) or with curcumin (0.125 μM (*B*) or 2 μM (*C*)). *D–E*, curcumin disaggregated preformed Aβ40 fibrils. Aβ40 (100 μg/ml) fibrils were incubated for 3 days at 37 °C and then further incubated with vehicle alone (*D*) or with curcumin (0.125 μM (*E*) or 2 μM (*F*)) for an additional 3 days at 37 °C. *Bar*, 2 μm. Original magnification was ×8900.

with a higher concentration of Aβ40 (100 μg/ml; Fig. 5*D*). These fibrils were extensive and more uniform in thickness than those at the lower concentration, with less branching, bumps, or nodules. In order to test whether low physiologically relevant concentrations of curcumin might inhibit fibril formation, we tested curcumin's impact on Aβ assembly at the lower Aβ40 (50 μg/ml) concentration. If a low dose of curcumin (0.125 μM) was included in the initial incubation, fibril formation appeared reduced (Fig. 5*B*). A higher dose (2 μM) resulted in similar but more potent inhibition of fibril formation (Fig. 5*C*). Droplets of curcumin/Tween accumulated with curcumin dose as fibril formation was inhibited.

In order to determine whether curcumin could also be inhibitory when added after initial aggregation events, we incubated 100 μg/ml Aβ40 for 3 days at 37 °C and then incubated another 3 days at 37 °C without (Fig. 5*D*) or with 0.125 μM (Fig. 5*E*) and 2 μM curcumin (Fig. 5*F*). The results show that curcumin limits fibril formation even when added midway through the incubation, consistent with an impact on fibril maturation or dissolution.

Curcumin Prevents Formation of Oligomers—Soluble oligomers of Aβ or "ADDLs" are a neurotoxic species implicated in AD pathogenesis (22–25). In order to test whether curcumin can block the formation of these neurotoxic oligomers, we dissolved Aβ40 and Aβ42 in HFIP to reconstitute "seedless" monomer and then incubated with and without curcumin in an oligomer formation protocol modified from Kayed *et al.* (19) and

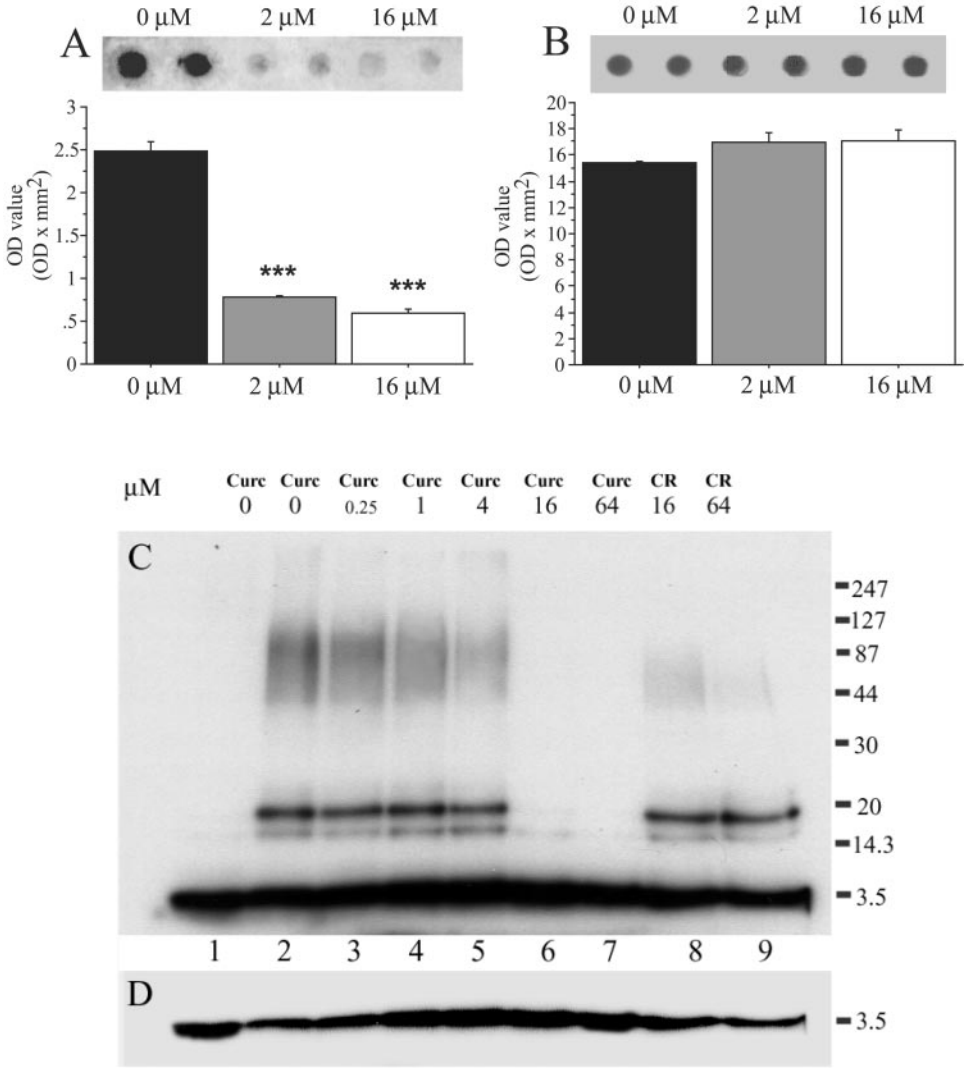

FIG. 6. **Curcumin inhibits formation of Aβ oligomers.** *A*, *scan* and *bar graph* of dot blot where Aβ40 oligomers were incubated with curcumin. Aβ40 oligomers (400 μg/ml) were incubated for 48 h at 25 °C. Curcumin was used at 0, 2, and 16 μM. Samples were immunoblotted as a dot blot and probed with A11 antibody, which is specific for oligomers. The dot blot was scanned and analyzed with Molecular Analyst, and one-way ANOVA was used to determine significance. ***, $p < 0.001$. The *error bars* represent S.E. *B*, scan and bar graph of dot blots from *A* probed with 6E10 antibody against Aβ (1:10,000). Dot blots were scanned and analyzed in a similar fashion. *C*, Western blot of Aβ42 oligomers and various doses of curcumin (*Curc*) and Congo Red (*CR*). Aβ42 (5 μM) was incubated at 37 °C for 4 h with curcumin, Congo Red, or no compound. Samples were centrifuged at 14,000 × g (4 °C for 10 min), and the supernatants were immunoblotted with 6E10 (1:2000). Bands at 3.5 kDa represent the monomeric Aβ form, whereas the smear between 44 and 127 kDa represents the oligomeric form of Aβ. *Lane 1*, Aβ42 monomer (no aggregation) only; *lanes 2–7*, Aβ42 and curcumin (0, 0.25, 1, 4, 16, and 64 μM); *lanes 8* and *9*, Aβ42 and CR (16 and 64 μM). *D*, Western blot of the 3.5-kDa monomeric Aβ band. This is a lighter exposure of the same blot seen in *C* and better illustrates the increase in monomer Aβ as curcumin dose increases.

Chromy *et al.* (18). The resulting oligomer-enriched supernatants were taken for analysis by dot blot and immunoblot with an oligomer-specific antibody A11 and 6E10. Dot blots showed dose-dependent inhibition of oligomer formation (Fig. 6*A*). When dot blots were probed with a non-oligomer-specific Aβ 6E10 antibody, there was no appreciable decrease in signal (Fig. 6*B*), indicating that the A11 signal was specific for oligomeric Aβ. One-way ANOVA analysis of A11 dot blot scans indicated that both 2 and 16 μM curcumin can significantly reduce Aβ oligomer formation ($p < 0.001$).

We then compared curcumin and Congo Red for their ability to block oligomer formation. Aβ42 (5 μM) was included to show the unaggregated monomeric form of Aβ (3.5 kDa; Fig. 6*C*, *lane 1*). When Aβ42 was allowed to aggregate without curcumin or CR, two bands between 14.3 and 20 kDa representing the 4–5-mer and an aggregated oligomer smear at 44–127 kDa were also present (*lane 2*). As the curcumin dose increased from 0 to 4 μM, the amount of higher molecular mass aggregated smear decreased as the amount of monomer Aβ increased (Fig. 6, *C* and *D*, *lanes 2–5*). When curcumin was present at 16 and 64 μM, the oligomeric Aβ bands (14.3–127 kDa) disappeared, whereas the monomeric Aβ (*lanes 6* and *7*) remained similar to the unaggregated Aβ in *lane 1*. At 16 and 64 μM, CR could reduce the oligomeric smear but not the 4–5-mer Aβ band. Together, these data imply that nontoxic curcumin can inhibit Aβ42 oligomer formation as well as or better than toxic CR.

Oligomeric-dependent toxicity was first determined using the oligomeric specific antibody A11 to block Aβ42 toxicity in APPSwe N2a cells (Fig. 7*A*). LDH release was measured after 72 h of incubation, and one-way ANOVA demonstrated a significant increase in LDH in cells incubated with oligomer Aβ alone ($p < 0.0001$). Incubating cells in conjunction with the A11 antibody resulted in a 42.7% reduction in toxicity, indicating that cell toxicity was dependent on the Aβ42 oligomers ($p < 0.0001$). To further evaluate whether curcumin can inhibit oligomer toxicity, Aβ42 oligomer (100 nM) with and without

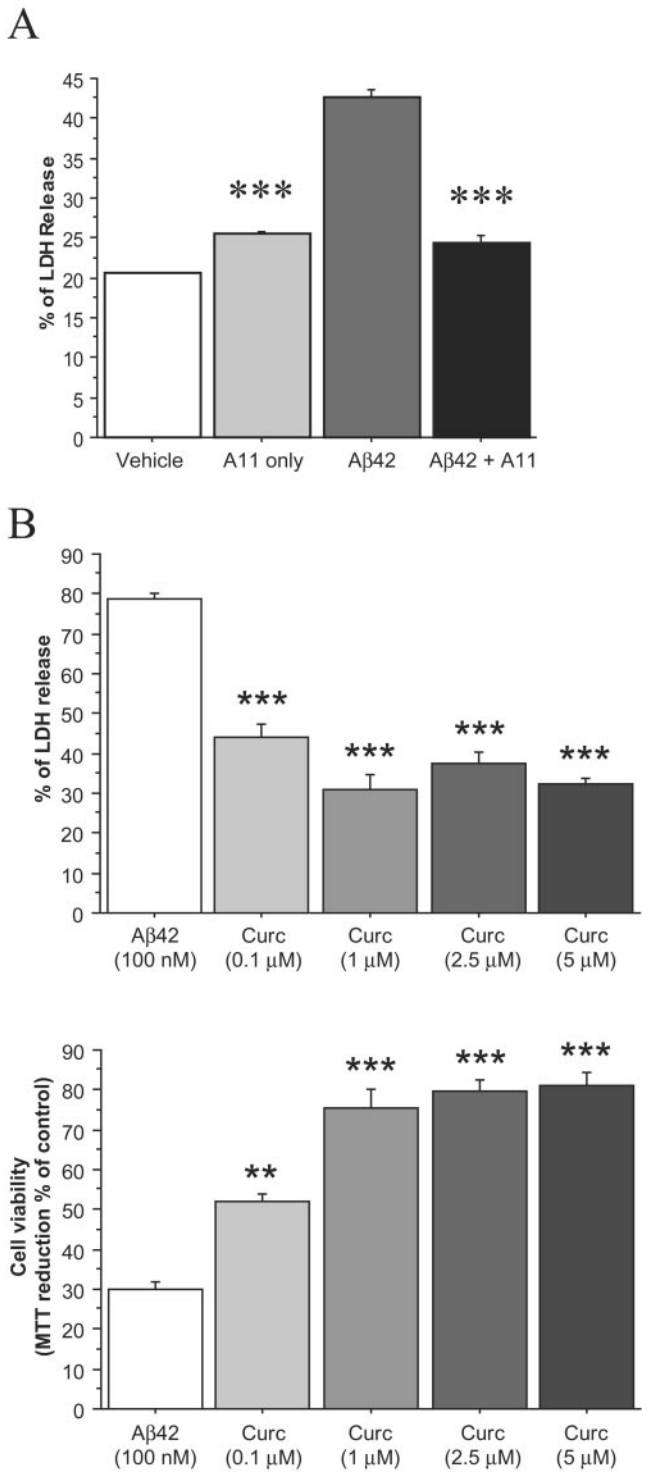

FIG. 7. **Curcumin (*Curc*) blocks toxicity of Aβ42 oligomer in differentiated SH-SY5Y neuroblastoma cells.** *A*, oligomer-dependent toxicity was first evaluated in N2a cells. Aβ42 (100 nM) was incubated with and without the oligomer-specific A11 antibody (1:500) for 72 h before medium was collected for LDH measurement. ***, $p < 0.0001$ when compared with Aβ42 alone. *B*, Aβ42 oligomer (100 nM) was added with or without curcumin (0–5 μM) to differentiated SY5Y cells for 48 h. The 3-(4,5-dimethylthiazol-2-yl)-2,5-diphenyltetrazolium bromide and LDH assays were used to determine cell viability and cell toxicity and were performed in triplicate. Data were analyzed by one-way ANOVA to evaluate treatment effect. ***, $p < 0.0001$ when compared with Aβ42 oligomer only. **, $p < 0.001$ when compared with Aβ42 oligomer only.

curcumin (0–5 μM) was added to differentiated SH-SY5Y neuroblastoma cells for 48 h before cell viability and toxicity were determined. One-way ANOVA analysis revealed a significant

TABLE I

Curcumin binds to peptide sequences that form fibrils or protofibrils

Shown are a schematic diagram and table of curcumin binding experiments. Aβ was aggregated for 10 days at 37 °C before an aliquot was removed for EM analysis. Curcumin was incubated with samples before they were centrifuged. Pellets were smeared on glass slides to check for Aβ binding while supernatants were applied to Tg2576 mouse brain sections for plaque labeling. Weak staining was defined as + or ++, and strong staining was +++ or ++++. Fibrils/protofibrils were determined by estimating thickness and length of fibers.

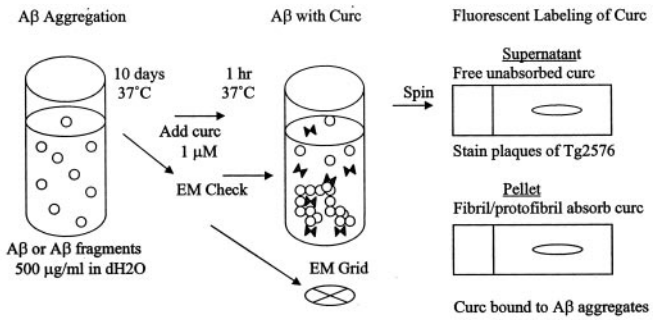

Peptide Sequence	Presence of fibrils/protofibrils?	Intensity of plaque labeling with supernatant
1-40 (dH_2O)	Fibrils	+
1-42 (dH_2O)	Fibrils	No staining
1-40 (HFIP)	Protofibrils	++
1-42 (HFIP)	Protofibrils	++
1-28	Protofibrils	+
12-28	Protofibrils	++
25-35	Protofibrils	+
1-13	None	++++
8-17	None	++++
14-24	None	++++
17-28	None	+++
17-24	None	++++
34-40	None	++++
37-42	None	++++
Curcumin only	None	++++

increase in cell viability with all curcumin doses (Fig. 7*B*). Moreover, this treatment effect was most effective at 0.1 and 1 μM curcumin, since the inhibitory effect appeared to plateau with 2.5 and 5 μM curcumin. Thus, these data indicate that curcumin inhibited cell toxicity of Aβ42 oligomers at 0.1 and 1 μM doses.

Fibril Conformation Required for Curcumin Binding—We have shown that curcumin can bind to plaques and block Aβ aggregation as well as fibril and oligomer formation. The molar ratios for successful Aβ fibril and aggregate inhibition by curcumin in the assays we used were clearly greater than 1:1, consistent with the idea that curcumin does not bind monomeric Aβ but rather to some secondary structure involved in later stages of assembly. Thus, we evaluated whether fibril formation or a specific sequence is necessary for curcumin binding. Various fragments of Aβ were incubated for 10 days at 37 °C to allow fibrils to form. These sequences are listed in Table I. An aliquot was removed for EM analysis before solutions were incubated with 1 μM curcumin. After centrifugation, supernatants were also applied to Tg2576 brain sections to label plaques. EM analysis demonstrated that with our conditions full-length Aβ40 and Aβ42 formed fibrils or protofibrils, depending on whether they were dissolved in dH_2O or HFIP (Table I). Shorter peptide sequences such as Aβ 1–28, 12–28, and 25–35 also had the ability to form fibrils that were fluorescently labeled by curcumin on slides (not shown). Plaque-labeling was markedly reduced or absent by preabsorption of curcumin with fibril-forming Aβ peptides (Aβ 12–28 and 25–35). In contrast, nonaggregating 17–28, a sequence containing the overlap of 12–28 and 25–35 did not absorb out or compete with curcumin plaque labeling. In fact, even full-length Aβ,

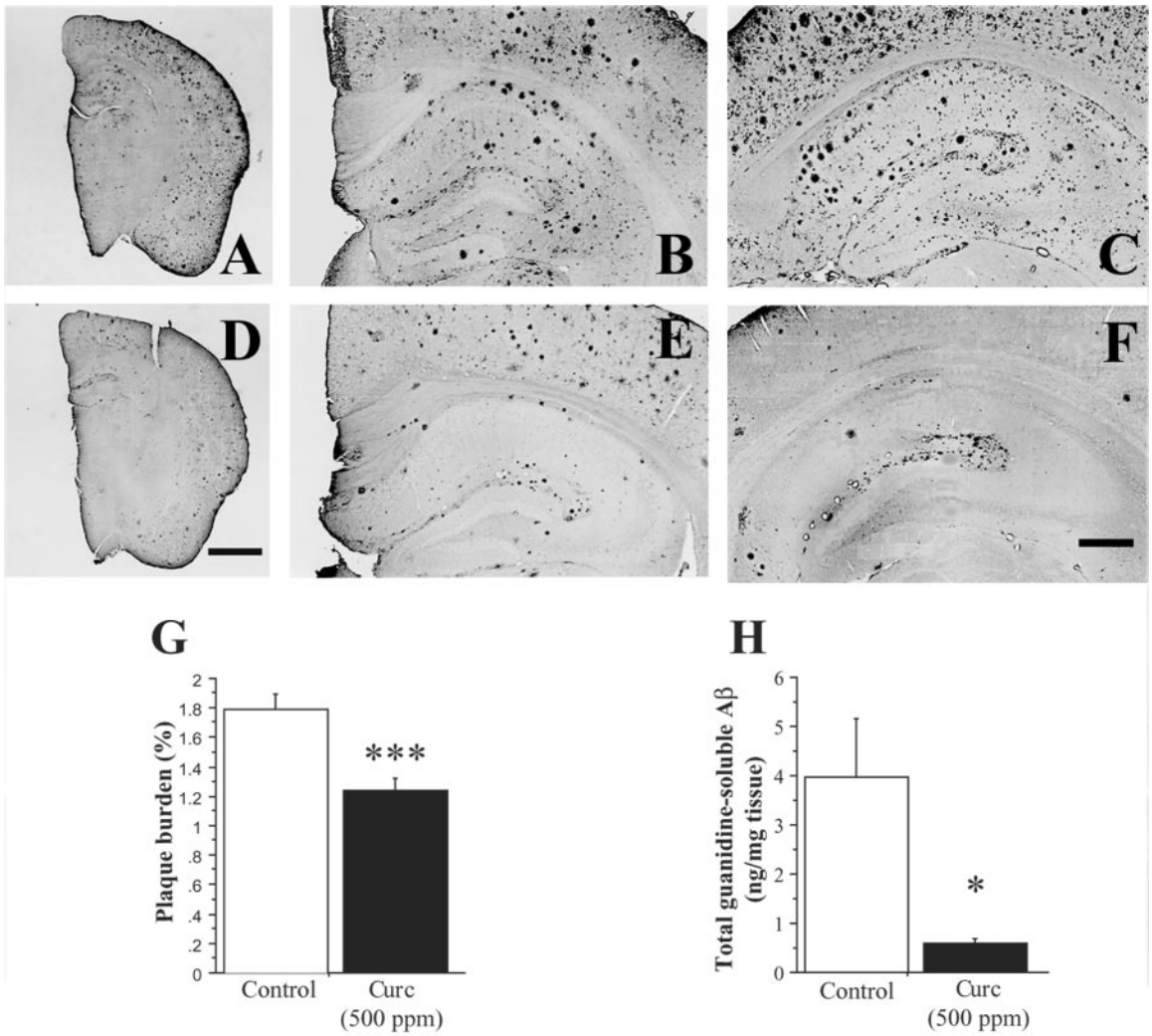

FIG. 8. **Curcumin suppresses amyloid accumulation in aged APP transgenic mice.** Tg2576 mice were placed on chow with ($n = 4$) or without 500 ppm curcumin ($n = 6$) at 17 months of age. At 22 months of age, brains were removed for histological and immunological measurement (ELISA) of amyloid. *A–F*, depict plaque burden analyzed from coronal sections through anterior and posterior hippocampus of control mice (*A–C*) and curcumin-treated mice (*D–F*). Representative photos of low magnification views show fewer amyloid deposits in curcumin mice (*D*) compared with control mice (*A*). *Bar*, 1 mm. This suppression can be easily seen with the higher magnification photos from anterior (*B* and *E*) and posterior hippocampal sections (*C* and *F*). *Bar*, 40 μm. Image analysis revealed a significant treatment effect, where plaque burden was reduced by 32.5% in curcumin-treated animals ($p < 0.0001$) (*G*). *H*, a *bar graph* of ELISA measurements of total guanidine-soluble Aβ showing an 85% reduction in Aβ levels with curcumin treatment. Samples of 5 M guanidine extracts were applied in triplicate, and data were square root-transformed to achieve quality of variance before subjection to one-way ANOVA. p values of <0.05 were considered significant.

when HFIP-monomerized, did not absorb out or compete with curcumin plaque labeling. A range of other shorter Aβ peptides (1–13, 8–17, 14–24, 17–24, 34–40, and 37–42) did not form fibrils, and preabsorption of the curcumin with these non-fibril-forming Aβ peptides had no effect on curcumin's plaque labeling. Taken together, these experiments argue that, like other amyloid dyes, curcumin binds Aβ only if it is aggregated (*i.e.* curcumin Aβ labeling does not depend on primary sequence alone but is dependent on aggregate-related structure).

Although we have shown that curcumin could limit amyloid accumulation in Aβ-infused rats and in Tg2576 mice when administered before extensive amyloid accumulation in Tg2576 mice (10–16 months old), other approaches that were successful in young APP transgenics have not been effective against the large amounts of deposited amyloid in older APP transgenics (26). Therefore, we tested curcumin's amyloid suppressing efficacy in a small cohort of Tg2576 with 500 ppm curcumin in chow beginning at 17 months, an age when amyloid accumulation is as great or greater than in human AD brain (27). Animals were sacrificed at 22 months of age, and brains were removed for histological and biochemical analysis. Coronal sections from control ($n = 6$) and curcumin mice ($n = 8$) were stained with an antibody against Aβ 1–13 (DAE). Plaque burden was visibly reduced throughout cortical and hippocampal areas in curcumin mice (Fig. 8, *D–F*) compared with control mice (Fig. 8, *A–C*). Statistical analysis revealed a significant reduction in plaque burden (−32.5%, $p < 0.0001$; Fig. 8*G*) and levels of the detergent-insoluble Aβ (−85%, $p = 0.02$; Fig. 8*H*). Thus, these data indicate that curcumin has potent antiamyloidogenic activity, even in aged animals.

DISCUSSION

The association of NSAID consumption with decreased AD risk is a consistent epidemiological finding (28–34). Potential mechanisms underlying apparent protection are being explored. A subset of NSAIDs (including ibuprofen) can directly lower Aβ42 production independently of cyclooxygenase inhibition and slow amyloid accumulation *in vivo* (35, 36). Curcumin has NSAID activities independent of cyclooxygenase inhibition (37–39) and reduces amyloid accumulation *in vivo* (12) but fails to reduce Aβ42 production *in vitro* (40). Thus, curcumin's amyloid suppressing function must stem from another

activity. A postproduction mechanism inhibiting Aβ aggregation is consistent with curcumin's suppression of Aβ deposition in rat models with chronic intraventricular infusion of exogenous human Aβ (41).

Selected NSAIDs, such as ibuprofen, naproxen, ketoprofen, and indomethacin, and various compounds can bind to amyloid and inhibit Aβ aggregation (42, 43). Aggregation inhibitors include Congo Red, its derivative chrysamine G, and RS-0406, a β-sheet breaker that inhibits Aβ42 fibrillogenesis and oligomer formation (14). CR can also bind to amyloid and block oligomer formation at low Aβ concentrations (9). Its fibril-binding properties are a result of a symmetrical sulfonated azodye structure with charge spaced across a hydrophobic bridge. This allows an alignment of CR molecules along the fibril axis with electrostatic interactions between the negative charges on CR and the positive charges on protonated antiparallel Aβ. This charge can be replaced by polar groups such as those present in chrysamine G, making it more brain-permeable than CR (10) (Fig. 1). RS-0406, which was selected by high throughput screening, has analogous polar groups spaced by a hydrophobic bridge. Curcumin is similar to CR, since it can also bind to plaques (Fig. 2), prevent oligomer formation at similar low ID_{50}, and recognize secondary structure in fibrillar and oligomeric Aβ. However, like chrysamine G, curcumin's symmetrical phenol groups make it more brain-permeable than CR and able to cross the blood-brain barrier to bind to plaques *in vivo* (Fig. 3).

Our ELISA and aggregation studies show that curcumin can inhibit aggregation or promote its disaggregation at low concentrations (IC_{50} = 0.81–1 μM; Fig. 4). Monomeric Aβ formed fewer aggregates in the presence of curcumin, whereas increasing doses of curcumin promoted disassembly of preformed Aβ aggregates. Ultrastructural evidence, illustrating fewer amyloid fibrils in curcumin-treated samples, supports anti-oligomer antibody and aggregation ELISA data with a completely different method. Sequences of Aβ that are instrumental in fibrillogenesis (*e.g.* full-length Aβ, Aβ 1–28, Aβ 12–28, and Aβ 25–35) are known (44–46). Our experiments also suggested that curcumin could bind and inhibit fibrils formed from these fibrillogenic sequences. Despite the common overlapping sequence of these fibrillogenic peptides being amino acids 25–28, curcumin cannot bind nonaggregating peptides that span this region (Aβ 17–28) (Table I). This would argue that curcumin's effects did not depend on Aβ sequence but on fibril-related conformation.

The aggregation ELISA demonstrates that curcumin inhibited Aβ aggregation better than the two NSAIDs ibuprofen and naproxen. Ibuprofen has been shown to inhibit more than 50% of the β-sheet conformation when 100 μM ibuprofen was incubated with 12.5 μM Aβ 25–35 (43). In our studies, doses as high as 16 μM ibuprofen or naproxen did not effectively inhibit aggregation. Levels for naproxen to directly block aggregation (32 μM) are probably not achievable in brain in the absence of toxicity.

Soluble Aβ oligomers are more diffusible than amyloid fibrils, highly toxic, and increasingly viewed as playing an important role in AD pathogenesis (22–25, 47). The observation that low micromolar or even submicromolar curcumin effectively blocks soluble Aβ oligomer formation and toxicity suggests curcumin's clinical potential to protect against oligomer-mediated synaptic or other neurotoxicity similar to RS-0406 *in vitro* (14). Consistent with this, oral curcumin reduced synaptic marker loss of central nervous system-infused exogenous Aβ (41). It is unclear whether a subset of other phenolic antioxidants found in plant extracts, including gingko biloba (18) and resveratrol from red wine might be similarly protective and potentially contribute to AD risk reduction (49) because of effects on Aβ aggregation.

A clinical trial of another drug known to inhibit Aβ aggregation has been performed using a compound (clioquinol) that inhibits zinc and copper ions from binding to Aβ (50). This raises the question as to whether the direct binding to β-amyloid, metal chelation, is another possible mechanism to account for curcumin-mediated reduction in Aβ aggregates and oxidative damage. Metals can promote Aβ aggregation, and clioquinol, a metal chelator of copper, zinc, and iron, has been shown to dramatically reduce Aβ deposits in the same Tg2576 line used in our study (51). Because metals like copper can bind Aβ at picomolar (Aβ 1–40) and even attomolar (Aβ 1–42) concentrations and promote aggregation, high affinity metal chelators can limit Aβ aggregation *in vitro* where most buffers have trace (~0.1 μM) copper (52). Thus, curcumin chelation of both iron and copper (but not zinc) has been proposed as one mechanism potentially contributing to amyloid reduction in animal models (53). In the latter report, spectrophotometrically detected curcumin copper binding reached half-maximum at ~3–12 μM copper with positive cooperativity, with K_{d1} ~10–60 μM and K_{d2} ~1.3 μM, well above the ~0.1 μM trace copper expected with *in vitro* buffers. As reviewed by Baum and Ng (53), it is not clear whether curcumin's avidity for copper and potential concentration in the brain will be high enough to directly alter central nervous system Aβ metal binding.

An efficacious drug must also be bioavailable and safe at the needed dose. We demonstrate that curcumin can prevent Aβ fibril formation at low doses in the 0.1–1 μM range, which is consistent with a recent *in vitro* report from Ono *et al.* (54). These doses can probably be achieved physiologically. Curcumin is rapidly glucuronidated after oral dosing, so plasma levels remain low, despite high intake. However, high oral curcumin dosing appears safe (*e.g.* 4–8-g doses in human patients produce no toxic effects, with peak serum curcumin levels of 0.51–1.77 μM) (55). Mouse brain curcumin levels of 0.41 μg/g (~1.1 μM) were measured 1 h after dosing that produced 0.6 μg/g (1.6 μM) in the plasma (56), suggesting that achievable brain levels may be close to blood levels. Curcumin-iron interaction reached half-maximum at ~2.5–5 μM iron and exhibited negative cooperativity, with K_{d1} ~0.5–1.6 μM and K_{d2} ~50–100 μM, suggesting that some iron chelation may be achieved at brain curcumin concentrations in the submicromolar range (53). We have found that oral curcumin treatment reduces central nervous system inducible nitric-oxide synthase, inflammatory cytokines, and lipid peroxidation (57). Brain levels of curcumin in the 0.1–1 μM range are similar to those required to inhibit central nervous system AP-1-mediated transcription *in vivo* (58) and related suppression of inducible nitric-oxide synthase, (59) and antioxidant activities. Curcumin can inhibit lipid peroxidation better than vitamin E (60), and it is a more potent antioxidant. Its IC_{50} value for Aβ aggregation is slightly below its IC_{50} value for lipid peroxidation (1.3 μM) (61, 62), indicating that curcumin would be effective at concentrations required for desirable antioxidant and anti-inflammatory activities. Whereas higher (>5 μM) doses of curcumin have been reported to inhibit multiple kinases and enzyme activities and bind metals, these phenomena are not likely to occur in brain with oral dosing. On the other hand, *in vitro* efficacy may not predict *in vivo* results. For example, whereas curcumin and another polyphenolic, rosmarinic acid, were found to inhibit Aβ aggregation *in vitro* (54), we find that rosmarinic acid actually increases Aβ accumulation in Aβ-infused rodent brain (63), which was in sharp contrast to curcumin's effect in the same model (41) and in our current *in vivo* results.

The final proof of any anti-amyloid effect is *in vivo* testing. Because amyloid accumulation begins decades before diagnosis, anti-amyloid therapy would ideally begin prior to clinical

symptoms. Approaches that remain efficacious at advanced stages of amyloid accumulation are clearly needed, and our *in vivo* observations suggest that curcumin may even be beneficial even after the disease has developed.

CONCLUSION

Curcumin is widely used at low doses as a yellow food dye and at higher doses in traditional Indian "Ayurvedic" medicine, typically as a turmeric extract. Because of its use as a food additive and its potential for cancer chemoprevention, curcumin has undergone extensive toxicological screening and preclinical investigation in rats, mice, dogs, and monkeys (11, 48). In clinical trials, cancer patients have not shown adverse effects with doses from 2000 to 8000 mg/day (55). Thus, our data showing low dose inhibition of amyloid oligomer and fibril formation as well as suppression in aged animals, combined with published antioxidant, anti-inflammatory, and antiamyloid activities in two animal models (15, 41), provide an increasingly compelling rationale for clinical trials for curcumin in the prevention or even treatment of AD.

REFERENCES

1. Selkoe, D. J. (1997) *Science* **275,** 630–631
2. Pike, C. J., Walencewicz, A. J., Glabe, C. G., and Cotman, C. W. (1991) *Brain Res.* **563,** 311–314
3. Klein, W. L., Krafft, G. A., and Finch, C. E. (2001) *Trends Neurosci.* **24,** 219–224
4. Cummings, J. L., Vinters, H. V., Cole, G. M., and Khachaturian, Z. S. (1998) *Neurology* **51,** S2–S17, S65–S67
5. Harris, M. E., Hensley, K., Butterfield, D. A., Leedle, R. A., and Carney, J. M. (1995) *Exp. Neurol.* **131,** 1–10
6. Puchtler, H., Sweat, F., and Levine, M. (1962) *J. Histochem. Cytochem.* **10,** 355–364
7. Lorenzo, A., and Yankner, B. A. (1994) *Proc. Natl. Acad. Sci. U. S. A.* **91,** 12243–12247
8. Abe, K., Kato, M., and Saito, H. (1997) *Neurosci. Res.* **29,** 129–134
9. Podlisny, M. B., Walsh, D. M., Amarante, P., Ostaszewski, B. L., Stimson, E. R., Maggio, J. E., Teplow, D. B., and Selkoe, D. J. (1998) *Biochemistry* **37,** 3602–3611
10. Klunk, W. E., Debnath, M. L., and Pettegrew, J. W. (1994) *Neurobiol. Aging* **15,** 691–698
11. Kelloff, G. J., Crowell, J. A., Hawk, E. T., Steele, V. E., Lubet, R. A., Boone, C. W., Covey, J. M., Doody, L. A., Omenn, G. S., Greenwald, P., Hong, W. K., Parkinson, D. R., Bagheri, D., Baxter, G. T., Blunden, M., Doeltz, M. K., Eisenhauer, K. M., Johnson, K., Knapp, G. G., Longfellow, D. G., Malone, W. F., Nayfield, S. G., Seifried, H. E., Swall, L. M., and Sigman, C. C. (1996) *J. Cell. Biochem. Suppl.* **26,** 72–85
12. Lim, G. P., Chu, T., Yang, F., Beech, W., Frautschy, S. A., and Cole, G. M. (2001) *J. Neurosci.* **21,** 8370–8377
13. Klunk, W. E., Jacob, R. F., and Mason, R. P. (1999) *Anal. Biochem.* **266,** 66–76
14. Nakagami, Y., Nishimura, S., Murasugi, T., Kaneko, I., Meguro, M., Marumoto, S. K., H., Koyama, K., and Oda, T. (2002) *Br. J. Pharamacol.* **137,** 676–682
15. Lim, G. P., Yang, F., Chu, T., Chen, P., Beech, W., Teter, B., Tran, T., Ubeda, O., Hsiao Ashe, K., Frautschy, S. A., and Cole, G. M. (2000) *J. Neurosci.* **20,** 5709–5714
16. Calon, F., Lim, G. P., Yang, F., Morihara, T., Teter, B., Ubeda, O., Rostaing, P., Triller, A., Salem, N., Jr., Ashe, K. H., Frautschy, S. A., and Cole, G. M. (2004) *Neuron* **43,** 633–645
17. Howlett, D. R., Perry, A. E., Godfrey, F., Swatton, J. E., Jennings, K. H., Spitzfaden, C., Wadsworth, H., Wood, S. J., and Markwell, R. E. (1999) *Biochem. J.* **340,** 283–289
18. Chromy, B. A., Nowak, R. J., Lambert, M. P., Viola, K. L., Chang, L., Velasco, P. T., Jones, B. W., Fernandez, S. J., Lacor, P. N., Horowitz, P., Finch, C. E., Krafft, G. A., and Klein, W. L. (2003) *Biochemistry* **42,** 12749–12760
19. Kayed, R., Head, E., Thompson, J. L., McIntire, T. M., Milton, S. C., Cotman, C. W., and Glabe, C. G. (2003) *Science* **300,** 486–489
20. Yang, F., Sun, X., Beech, W., Teter, B., Wu, S., Sigel, J., Vinters, H. V., Frautschy, S. A., and Cole, G. M. (1998) *Am. J. Pathol.* **152,** 379–389
21. Mosmann, T. (1983) *J. Immunol. Methods* **65,** 55–63
22. Walsh, D. M., Klyubin, I., Fadeeva, J. V., Cullen, W. K., Anwyl, R., Wolfe, M. S., Rowan, M. J., and Selkoe, D. J. (2002) *Nature* **416,** 535–539
23. Selkoe, D. J. (2002) *Science* **298,** 789–791
24. Gong, Y., Chang, L., Viola, K. L., Lacor, P. N., Lambert, M. P., Finch, C. E., Krafft, G. A., and Klein, W. L. (2003) *Proc. Natl. Acad. Sci. U. S. A.* **100,** 10417–10422
25. Lambert, M. P., Barlow, A. K., Chromy, B. A., Edwards, C., Freed, R., Liosatos, M., Morgan, T. E., Rozovsky, I., Trommer, B., Viola, K. L., Wals, P., Zhang, C., Finch, C. E., Krafft, G. A., and Klein, W. L. (1998) *Proc. Natl. Acad. Sci. U. S. A.* **95,** 6448–6453
26. Das, P., Murphy, M. P., Younkin, L. H., Younkin, S. G., and Golde, T. E. (2001) *Neurobiol. Aging* **22,** 721–727
27. Kawarabayashi, T., Younkin, L. H., Saido, T. C., Shoji, M., Hsiao-Ashe, K., and Younkin, S. G. (2001) *J. Neurosci.* **21,** 372–381
28. in't Veld, B. A., Ruitenberg, A., Hofman, A., Launer, L. J., van Duijn, C. M., Stijnen, T., Breteler, M. M., and Stricker, B. H. (2001) *N. Engl. J. Med.* **345,** 1515–1521
29. Etminan, M., Gill, S., and Samii, A. (2003) *Br. Med. J.* **327,** 128
30. Launer, L. J. (2003) *J. Am. Med. Assoc.* **289,** 2865–2867; Correction (2003) *J. Am. Med. Assoc.* **290,** 1154
31. Landi, F., Cesari, M., Onder, G., Russo, A., Torre, S., and Bernabei, R. (2003) *Am. J. Geriatr. Psychiatry* **11,** 179–185
32. Anthony, J. C., Breitner, J. C., Zandi, P. P., Meyer, M. R., Jurasova, I., Norton, M. C., and Stone, S. V. (2000) *Neurology* **54,** 2066–2071
33. In't Veld, B. A., Launer, L. J., Hoes, A. W., Ott, A., Hofman, A., Breteler, M. M., and Stricker, B. H. (1998) *Neurobiol. Aging* **19,** 607–611
34. Zandi, P. P., Anthony, J. C., Hayden, K. M., Mehta, K., Mayer, L., and Breitner, J. C. (2002) *Neurology* **59,** 880–886
35. Weggen, S., Eriksen, J. L., Das, P., Sagi, S. A., Wang, R., Pietrzik, C. U., Findlay, K. A., Smith, T. E., Murphy, M. P., Bulter, T., Kang, D. E., Marquez-Sterling, N., Golde, T. E., and Koo, E. H. (2001) *Nature* **414,** 212–216
36. Gasparini, L., Rusconi, L., Xu, H., del Soldato, P., and Ongini, E. (2004) *J. Neurochem.* **88,** 337–348
37. Chun, K. S., Keum, Y. S., Han, S. S., Song, Y. S., Kim, S. H., and Surh, Y. J. (2003) *Carcinogenesis* **24,** 1515–1524
38. Surh, Y. J., Chun, K. S., Cha, H. H., Han, S. S., Keum, Y. S., Park, K. K., and Lee, S. S. (2001) *Mutat. Res.* **480,** 243–268
39. Plummer, S. M., Holloway, K. A., Manson, M. M., Munks, R. J., Kaptein, A., Farrow, S., and Howells, L. (1999) *Oncogene* **18,** 6013–6020
40. Sagi, S. A., Weggen, S., Eriksen, J., Golde, T. E., and Koo, E. H. (2003) *J. Biol. Chem.* **278,** 31825–31830
41. Frautschy, S. A., Hu, W., Miller, S. A., Kim, P., Harris-White, M. E., and Cole, G. M. (2001) *Neurobiol. Aging* **22,** 991–1003
42. Agdeppa, E. D., Kepe, V., Petri, A., Satyamurthy, N., Liu, J., Huang, S. C., Small, G. W., Cole, G. M., and Barrio, J. R. (2002) *Neuroscience* **117,** 723–730
43. Thomas, T., Nadackal, T. G., and Thomas, K. (2001) *Neuroreport* **12,** 3263–3267
44. Liu, R., McAllister, C., Lyubchenko, Y., and Sierks, M. R. (2004) *J. Neurosci. Res.* **75,** 162–171
45. Legleiter, J., Czilli, D. L., Gitter, B., DeMattos, R. B., Holtzman, D. M., and Kowalewski, T. (2004) *J. Mol. Biol.* **335,** 997–1006
46. Pike, C. J., Walencewicz-Wasserman, A. J., Kosmoski, J., Cribbs, D. H., Glabe, C. G., and Cotman, C. W. (1995) *J. Neurochem.* **64,** 253–265
47. Wang, J., Asensio, V. C., and Campbell, I. L. (2002) *Curr. Top. Microbiol. Immunol.* **265,** 23–48
48. Chainani-Wu, N. (2003) *J. Altern. Complement Med.* **9,** 161–168
49. Han, Y. S., Zheng, H., W., Bastianetto, S., Chabot, J. G., and Quirion, R. (2004) *Br. J. Pharmacol.* **141,** 997–1005
50. Ritchie, C. W., Bush, A. I., Mackinnon, A., Macfarlane, S., Mastwyk, M., MacGregor, L., Kiers, L., Cherny, R., Li, Q. X., Tammer, A., Carrington, D., Mavros, C., Volitakis, I., Xilinas, M., Ames, D., Davis, S., Beyreuther, K., Tanzi, R. E., and Masters, C. L. (2003) *Arch. Neurol.* **60,** 1685–1691
51. Cherny, R. A., Atwood, C. S., Xilinas, M. E., Gray, D. N., Jones, W. D., McLean, C. A., Barnham, K. J., Volitakis, I., Fraser, F. W., Kim, Y., Huang, X., Goldstein, L. E., Moir, R. D., Lim, J. T., Beyreuther, K., Zheng, H., Tanzi, R. E., Masters, C. L., and Bush, A. I. (2001) *Neuron* **30,** 665–676
52. Atwood, C. S., Scarpa, R. C., Huang, X., Moir, R. D., Jones, W. D., Fairlie, D. P., Tanzi, R. E., and Bush, A. I. (2000) *J. Neurochem.* **75,** 1219–1233
53. Baum, L., and Ng, A. (2004) *J. Alzheimers Dis.* **6,** 367–377, 443–449
54. Ono, K., Hasegawa, K., Naiki, H., and Yamada, M. (2004) *J. Neurosci. Res.* **75,** 742–750
55. Cheng, A. L., Hu, C. H., Lin, J. K., Hsu, M. M., Ho, Y. F., Shen, T. S., Ko, J. Y., Lin, J. T., Lin, B. R., Ming-Shiang, W., Yu, H. S., Jee, S. H., Chen, G. S., Chen, T. M., Chen, C. A., Lai, M. K., Pu, Y. S., Pan, M. H., Wang, Y. J., Tsai, C. C., and Hsieh, C. Y. (2001) *Anticancer Res.* **21,** 2895–2900
56. Pan, M. H., Huang, T. M., and Lin, J. K. (1999) *Drug Metab. Dispos.* **27,** 486–494
57. Cole, G. M., Yang, F., Lim, G. P., Cummings, J. L., Masterman, D. L., and Frautschy, S. A. (2003) *Curr. Med. Chem.* **3,** 15–25
58. Luo, Y., Hattori, A., Munoz, J., Qin, Z., and Roth, G. (1999) *Mol. Pharmacol.* **56,** 254–264
59. Chan, M. M., Huang, H. I., Fenton, M. R., and Fong, D. (1998) *Biochem. Pharmacol.* **55,** 1955–1962
60. Zhao, B. L., Li, X. J., He, R. G., Cheng, S. J., and Xin, W. J. (1989) *Cell Biophys.* **14,** 175–185
61. Soudamini, K. K., Unnikrishnan, M. C., Soni, K. B., and Kuttan, R. (1992) *(1992) Indian J. Physiol. Pharmacol.* **36,** 239–243
62. Sreejayan, and Rao, M. N. A. (1994) *J. Pharm. Pharmacol.* **46,** 1013–1016
63. Frautschy, S. A., Hammer, H., Hu, S., Hu, W., Oh, M., Miller, S. A., Lim, G. P., Harris-White, M. E., and Tenner, A. J. (2003) *Soc. Neurosci. Abstr.* 667.12